Published online 10 May 2016

Nucleic Acids Research, 2016, Vol. 44, No. 14 ***6935–6948***
doi: 10.1093/nar/gkw404

Protection against deleterious nitrogen compounds: role of σ^S-dependent small RNAs encoded adjacent to *sdiA*

Yue Hao†, Taylor B. Updegrove†, Natasha N. Livingston and Gisela Storz*

Division of Molecular and Cellular Biology, Eunice Kennedy Shriver National Institute of Child Health and Human Development, Bethesda, MD 20892-5430, USA

Received March 15, 2016; Revised April 30, 2016; Accepted May 02, 2016

ABSTRACT

Here, we report the characterization of a set of small, regulatory RNAs (sRNAs) expressed from an *Escherichia coli* locus we have denoted *sdsN* located adjacent to the LuxR-homolog gene *sdiA*. Two longer sRNAs, $SdsN_{137}$ and $SdsN_{178}$ are transcribed from two σ^S-dependent promoters but share the same terminator. Low temperature, rich nitrogen sources and the Crl and NarP transcription factors differentially affect the levels of the SdsN transcripts. Whole genome expression analysis after pulse overexpression of $SdsN_{137}$ and assays of *lacZ* fusions revealed that the $SdsN_{137}$ directly represses the synthesis of the nitroreductase NfsA, which catalyzes the reduction of the nitrogroup (NO_2) in nitroaromatic compounds and the flavohemoglobin HmpA, which has aerobic nitric oxide (NO) dioxygenase activity. Consistent with this regulation, $SdsN_{137}$ confers resistance to nitrofurans. In addition, $SdsN_{137}$ negatively regulates synthesis of NarP. Interestingly, $SdsN_{178}$ is defective at regulating the above targets due to unusual binding to the Hfq protein, but cleavage leads to a shorter form, $SdsN_{124}$, able to repress *nfsA* and *hmpA*.

INTRODUCTION

In order to survive in many different, constantly-changing environments, bacteria have intricate mechanisms to sense environmental cues and increase or decrease the levels of the appropriate proteins and enzymes at the transcriptional and/or post-transcriptional levels. Key post-transcriptional regulators are small RNAs (sRNAs), typically 50 to 300 nucleotides in length, that base pair with mRNAs encoded in *trans* at a distinct genomic location (1,2). By base pairing at or near the ribosome-binding site, the sRNAs can block translation. These sRNAs can also activate translation when base pairing results in a change in mRNA secondary structure that liberates a ribosome binding site. In addition, base pairing can lead to the recruitment of RNase E either in conjunction with or independent of effects on ribosome binding. Given the limited complementarity to their target mRNAs, the sRNAs in a number of bacteria including *Escherichia coli* require the RNA chaperone Hfq to stabilize the sRNAs and facilitate sRNA–mRNA duplex formation (3,4).

Many base pairing sRNAs are induced in response to very specific environmental signals and then act to protect the cells and/or make maximal use of limited resources under these conditions. For example, RyhB, whose levels are induced by conditions of iron starvation, represses the synthesis of non-essential iron-storage and iron-utilization proteins (5). Similarly, FnrS RNA, whose levels are induced by oxygen limitation, represses the synthesis of proteins that are not needed under anaerobic conditions (6,7). Three σ^E-dependent sRNAs, RybB, MicA and MicL, that are all induced by cell envelope stress, repress the synthesis of all abundant outer membrane proteins thus allowing chaperones required for the insertion of new proteins to be redirected to misfolded cell envelope proteins (8).

Expression of a number of sRNAs is highest in stationary phase (9), conditions under which bacteria undergo substantial changes in morphology and physiology to conserve energy and become resistant to starvation and various environmental stresses. The key regulator in stationary phase is σ^S, encoded by the *rpoS* gene (10,11). This alternative sigma factor directs the expression of hundreds of genes when cells enter stationary phase or encounter other stresses, alone at some promoters and in conjunction with additional transcription factors at other promoters. The GadY, SraL and

*To whom correspondence should be address. Tel: +1 301 4020968; Fax: +1 301 4020078; Email: storz@helix.nih.gov
†These authors contributed equally to this paper as first authors.
Present addresses:
Yue Hao, Institute of Apicultural Research, Chinese Academy of Agricultural Sciences, Beijing 100093, China.
Taylor B. Updegrove, Laboratory of Molecular Biology, National Cancer Institute, Bethesda, MD 20892, USA.
Natasha N. Livingston, Food and Drug Administration Center for Tobacco Products, Silver Spring, MD 20993, USA.

SdsR sRNAs have been shown to be σ^S-dependent sRNAs (12–14). GadY, positively regulates the expression of GadX and GadW, two transcription factors controlling the acid response, by directing cleavage of the *gadXW* mRNA to give more stable products (13,15). SraL was found to down-regulate the expression of the *tig* gene, which encodes the chaperone Trigger Factor involved in protein folding (14). SdsR acts as a repressor by base pairing with the coding region of *mutS* encoding a component of the methyl-directed mismatch repair complex and the 5′UTR of *tolC* encoding an outer membrane porin in *E. coli* (16,17). In *Salmonella*, SdsR also represses synthesis of the major porin OmpD by basepairing with the coding region of the *ompD* mRNA (12).

Here, we report on another σ^S-dependent sRNA in *E. coli*, SdsN, which is induced in stationary phase, particularly when cells are grown at low temperature or with preferred nitrogen sources, and regulates the levels of the nitrate- and nitrite-responsive NarP transcription factor as well as enzymes that metabolize oxidized nitrogen compounds.

MATERIALS AND METHODS

Bacterial strains and plasmids

The strains and plasmids used in this study are given in Supplementary Tables S1 and S2, respectively. *E. coli* K-12 MG1655 was employed as the wild-type (WT) strain. Phage λ Red-mediated recombineering was used to construct deletion alleles marked by Km^R flanked by FRT (FLP recognition target) sites, which were amplified using pKD13 as template for PCR (18). After P1 transduction into MG1655, the Km^R cassette was removed by introduction of the FLP expression plasmid pCP20. Other alleles were transduced from previously published strains (19,20). The *nfsA-lacZ*, *hmpA-lacZ* and *narP-lacZ* translational fusions were created as described (21); the first nine codons of *nfsA* and *hmpA*, or the first 30 codons of *narP* as well as the entire 5′-UTR of each gene were PCR amplified and fused to *lacZ* driven by an arabinose-inducible pBAD promoter. SdsN derivatives were overexpressed from the pBRplac plasmid (22). The $sdsN_{178}$, $sdsN_{137}$ and $sdsN_{124}$ fragments were PCR amplified from MG1655 chromosomal DNA, digested with EcoRI and AatII, and cloned into the corresponding sites of pBRplac. The mutant derivatives of the *lacZ* fusions and SdsN-overexpression plasmids were generated by overlapping PCR and introduced into the chromosome or pBRplac as described above. All plasmid and chromosomal constructs were verified by DNA sequencing. Primers used for PCR and sequencing are listed in Supplementary Table S3.

Growth conditions

Unless indicated otherwise, bacterial strains were grown overnight with shaking at 37°C in Luria Broth (LB) or M63 with 0.2% glucose media, both supplemented with standard concentrations of the appropriate antibiotics, and then diluted ($OD_{600} \approx 0.02$–0.03) into the same medium. For the nitrofurazone sensitivity assays, back-diluted cultures were grown to $OD_{600} \approx 0.3$ in LB or for 14 h in M63 glucose. Half of each culture was challenged with 1 or 2 mM nitrofurazone (Sigma) or azomycin (Sigma) for 1 h after which 100 μl of 10^{-5}-dilutions of the LB cultures and 10^{-6}-dilutions of the M63 glucose cultures were plated on LB agar.

RNA extraction

Total RNA was isolated by extraction with hot acid phenol (23) or TRIzol Reagent (Ambion). For the hot acid phenol extraction, RNA was isolated from 750 μl of LB-grown cells or 10 ml of cells grown in M63 glucose, collected and resuspended in 700 μl of M63. For both types of samples, the cells were mixed with 500 μl of acid-phenol-chloroform (Ambion) and 102 μl of cell lysis solution (320 mM sodium acetate, 8% SDS and 16 mM EDTA) and incubated 15 min at 65°C. Supernatants were transferred to a new tube containing pre-heated 500 μl of acid-phenol-chloroform and incubated at 65°C for another 15 min. RNA was precipitated with 700 μl of 100% ethanol. For the TRIzol extraction, total cellular RNA was isolated from ∼5–10 OD_{600} of cells according to the manufacturer's instructions. RNA was precipitated by combining the ∼0.6 ml of the top aqueous phase with 0.5 ml isopropyl alcohol. For both extraction methods, precipitated RNA pellets were washed with 70% ethanol and resuspended in nuclease-free water. Total RNA concentrations were determined using a NanoDrop (Thermo Scientific).

Northern analysis

Total RNA (10 μg) was separated on a 8% polyacrylamide-7M urea gel in 1X TBE (90 mM Tris-borate 2 mM EDTA). The RNA was transferred to a Zeta-Probe GT blotting membrane (Bio-Rad) at 20V for ∼16 h at 4°C in 0.5X TBE. After transfer, membranes were allowed to dry, UV cross-linked on both sides, and incubated overnight at 45°C in UltraHyb (Ambion) hybridization buffer and oligonucleotides 5′-end-labeled with ^{32}P-ATP with T4 polynucleotide kinase (New England Biolabs). Subsequently, membranes were washed once with 2X SSC (150 mM NaCl 15 mM sodium citrate) 0.1%SDS, incubated 10 min at 45°C in 2X SSC 0.1%SDS, and washed 5X with 0.2X SSC 0.1% SDS. After washing, air-dried membranes were exposed to HyBlot CL film (Denville Scientific) at −80°C.

Primer extension analysis

Primer extension assays were carried out as previously described (24). Briefly, RNA samples (5 μg of total RNA) were incubated with 2 pmol of 5′-^{32}P -end-labeled primer at 80°C and then slow-cooled to 42°C. After the addition of dNTPs (1 mM each) and AMV reverse transcriptase (10 U, Life Sciences Advanced Technologies Inc.), the reactions were incubated in a 10 μl reaction volume at 42°C for 1 h. Reactions were terminated by adding 10 μl of Gel Loading Buffer II (Ambion). The DNA sequencing ladder was generated using Thermo Sequenase^{TM} Dye Primer Manual Cycle Sequencing Kit (Affymetrix) and an *sdsN* or *sdiA* PCR fragment. The cDNA products and sequencing ladder were fractionated on an 8% polyacrylamide urea sequencing gel containing 8 M urea in 1X TBE buffer at 70 W for 70 min.

The gel was dried and imaged using a STORM 840 (Amersham Biosciences).

Terminator-5′-phosphate-dependent exonuclease (TDE) digestion

Total RNA (7 μg) extracted from MG1655 cells grown to $OD_{600} \approx 5$ at 25°C in LB or 20 h at 37°C in M63 glucose were placed in two RNase-free 1.5 ml tubes; the sample in one was treated with TDE (Epicentre) while the second sample was incubated with buffer as described (8).

In vitro RNA synthesis

The *narP*, *hmpA*, $SdsN_{137}$ and $SdsN_{178}$ RNAs were synthesized using Megascript T7 kit (Ambion). $SdsN_{137}$ and $SdsN_{178}$ RNA were 5′-end-labeled with ^{32}P by treating the RNA with alkaline phosphatase (New England Biolabs) and then T4 polynucleotide kinase. ^{32}P-labeled RNAs were purified from 8% polyacrylamide-7M urea gels by excising and crushing the bands in RNA elution buffer (0.1 M sodium acetate, 0.1% SDS and 10 mM EDTA). The elution was extracted with an equal volume of phenol:chloroform:IAA (Invitrogen). The RNA was then ethanol precipitated, re-suspended in nuclease free dH_2O and quantified using the NanoDrop.

In vitro RNA structure probing

^{32}P-labeled $SdsN_{137}$ or $SdsN_{178}$ (∼2 nM) was incubated with purified Hfq (or equal volume of buffer) and 1 μg of yeast RNA (Ambion) in 1X RNA structure buffer (Ambion) in a total volume of 8 μl at 37°C for 15 min. Samples were mixed with RNase T1 (0.02 U, Ambion) or an equal volume of buffer and incubated at 37°C for 6 min. Inactivation/Precipitation Buffer (20 μl, Ambion) was added, and samples were placed at −80°C for ∼30 min. RNA pellets were collected by centrifugation, washed with 100 μl of 70% ethanol, air-dried and dissolved in 7 μl Gel Loading Buffer II. For the hydroxide (OH) ladder, 1 μl of ^{32}P-labeled $SdsN_{137}$ or $SdsN_{178}$ in 9 μl Alkaline Hydrolysis Buffer (Ambion) was incubated 5 min at 90°C. For the RNase T1 ladder, 1 μl of ^{32}P-labeled $SdsN_{137}$ or $SdsN_{178}$ in 9 μl Sequencing Buffer (Ambion) was denatured by incubating at 95°C for 1 min followed by cooling to 37°C. RNase T1 (0.1 U) was added, and the sample was incubated for 5 min at 37°C. For both ladders, the reactions were stopped by adding 12 μl of Gel Loading Buffer II. Samples (2 μl) were run on a 8% polyacrylamide-7M urea sequencing gel in 1X TBE. The gel was transferred onto Whatman filter paper, dried at 80° for 1 h, and imaged using the STORM 840.

Electrophoretic mobility shift assays (EMSA)

^{32}P-labeled $SdsN_{137}$ or $SdsN_{178}$ RNA (4 nM) was incubated at 37°C for 15 min with purified Hfq and 1 μg of yeast RNA in 1X RNA Structure Buffer in a total volume of 10 μl. For some samples, 1 μl 1X RNA Structure Buffer or unlabeled *hmpA* or *narP* RNA diluted in 1X RNA Structure Buffer was added and samples were incubated at room temperature for an additional 1 h. After the indicated incubation, 2.5 μl of non-denaturing RNA loading buffer (100 mM NH_4Cl, 50 mM NaCl, 50 mM KCl, 20 mM Tris-HCl, pH 8 and 50% glycerol) was added to each sample. Samples were then separated at 100 V on a native 6% polyacrylamide gel (37.5:1 Bis-Acrylamide, National Diagnostics) at 4°C in pre-chilled 0.5X TBE. Gels were imaged using the STORM 840.

Microarray analysis

MG1655 cells harboring pBR, pBR-$SdsN_{137}$ or pBR-$SdsN_{178}$ were grown to $OD_{600} \approx 0.4$ in LB at 37°C, then cells were induced with 100 μM isopropyl β-D-1-thiogalactopyranoside (IPTG) for 5 min. Cells were harvested and total RNA was isolated by hot-phenol method. Chromosomal DNA was removed with DNase I treatment before cDNA synthesis and hybridization of cDNA to the Affymetrix *E. coli* Genome2.0 array was carried according to the instructions in Affymetrix manual.

Immunoblot analysis

Cells collected from 1 ml of culture were resuspended in 80 μl/ OD_{600} 1X SDS PAGE loading buffer containing 5% β-mercaptoethanol, heated for 20 min at 95°C and then loaded onto a 4–15% Tris-Glycine gel (BioRad). Proteins were transferred onto a nitrocellulose membrane (Invitrogen) at 100 V for 1 h at 4°C in 1X Tris-glycine-SDS running buffer (KD Medical) with 20% methanol. Membranes were blocked 1 h at room temperature in 1X PBST (phosphate buffer saline with Tween20, Corning) with 5% milk and then probed with a 1:4000 dilution of α-RpoS antibody (provided by Susan Gottesman, NCI) for ∼16 h at 4°C. After three washes in 1X PBST, membranes were incubated with a 1:5000 dilution of HRP-anti-rabbit IgG (Sigma) for 1 h at room temperature. After three additional washes, membranes were developed using SuperSignal® West Pico Chemiluminescent Substrate (Thermo Scientific) and exposed to HyBlot CL film.

β-galactosidase assays

Three or four individual colonies from the indicated *lacZ* translational fusions transformed with pBR plasmids were grown overnight at 37°C in LB media containing 100 μg/ml ampicillin, diluted to an $OD_{600} = 0.03$ into fresh LB media with 100 μg/ml of ampicillin and 0.2% arabinose (to induce *lacZ* expression). IPTG (100 μM or 1 mM) was simultaneously added to some of the samples to induce expression from the pBR plasmids. Cells were grown to $OD_{600} \approx 0.5$ or 1.0 and then lysed in 700 μl of Z buffer containing 0.002% SDS and 30 μl chloroform. β-galactosidase activity levels were assayed as described before (6).

RESULTS

Multiple sRNA species are transcribed from the *sdiA-tcyN* intergenic region

Microarray analysis of RNAs that co-immunoprecipitate with Hfq in *E. coli* suggested an sRNA bound by Hfq was encoded in the intergenic region between *sdiA*, the gene

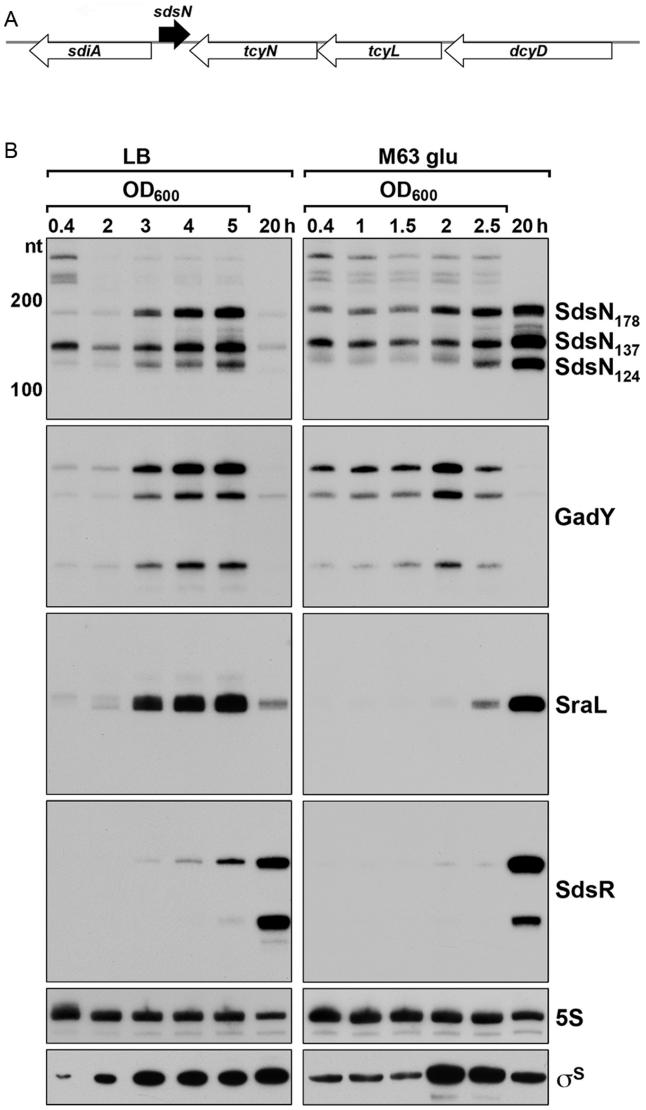

Figure 1. SdsN expression increases in stationary phase. (**A**) Schematic of region encompassing *sdsN*. The gene encoding SdsN (shaded in black) is located between *tcyN* (formerly *yecC*), encoding the ATP binding subunit of an L-cystine/L-cysteine ABC transporter complex and *sdiA*, encoding the LuxR homolog DNA binding transcription regulator. Transcription of *sdsN* is opposite both *tcyN* and *sdiA*. (**B**) Expression of SdsN, GadY, SraL and SdsR across growth in LB rich and M63 glucose minimal medium. Total RNA was isolated from wild-type (WT) MG1655 grown in LB or M63 media at 37°C for the indicated OD_{600} or time points. The RNA (10 μg) was separated on an 8% polyacrylamide-7M urea gel, transferred to a nitrocellulose membrane and probed with a ^{32}P-labelled oligonucleotide specific for each sRNA or 5S as control. σ^S levels were assayed by immunoblot analysis of cells taken simultaneously.

for a LuxR-family transcription regulator that serves as a 'suppressor of the cell division inhibitor', and *tcyN* (formerly *yecC*), the gene for the ATP binding subunit of an L-cystine/L-cysteine ABC transporter (Figure 1A), but no signal was detected by northern analysis under the conditions examined (25). Recent deep sequence analysis of the *E. coli* transcriptome again showed a small transcript is encoded in the *sdiA-tcyN* intergenic region (26,27). To obtain further information about the expression of this putative sRNA, we probed the total RNA isolated from *E. coli* MG1655 grown to different stages in LB rich medium and M63 glucose minimal medium at 37°C (Figure 1B). We now detected multiple transcripts, particularly in stationary phase. The two most prominent bands were ∼140 nt ($SdsN_{137}$) and ∼180 nt ($SdsN_{178}$), with the highest levels at $OD_{600} \approx 5$ in LB medium and after 20 h of growth in M63 glucose medium. A number of additional bands were also observed for both samples. Probing with a downstream oligonucleotide showed that the longest transcripts prevalent early in growth are 3′ extensions of the major transcripts (Supplementary Figure S1A). In contrast, the shorter transcripts of ∼120 nt ($SdsN_{124}$) lack the 5′ end. These smaller RNAs accumulate in late stationary phase, especially in M63 glucose medium.

The 5′ ends of the ∼140 and ∼180 nt transcripts were mapped by primer extension analysis (Supplementary Figure S1B) and examination of transcriptomic promoter mapping data (27). While multiple 5′ ends were detected by both approaches, the promoter mapping data indicate the prominent bands correspond to transcripts of 137 and 178 nt that share the same Rho-independent terminator (Figure 2A). Both forms were not fully digested by terminator exonuclease from RNA extracted from cells grown in LB and M63 glucose media (Supplementary Figure S1C), unlike the complete digestion observed for the processed derivative of SdsR. Thus, $SdsN_{178}$ and $SdsN_{137}$ likely have 5′-triphosphates consistent with transcription from two distinct promoters. The 5′ end of the ∼120 nt transcript was also mapped by primer extension analysis, which showed that one form is 124 nt (Supplementary Figure S1B). This band is no longer detected upon terminator exonuclease treatment indicating it is derived by processing (Supplementary Figure S1C).

We also monitored the induction of the *sdsN* promoter by integrating the *lacZ* reporter gene downstream of both the $sdsN_{137}$ and $sdsN_{178}$ promoters. Expression of this P_{sdsN}-*lacZ* fusion was low in exponential phase and increased in stationary phase, particularly in cells grown at lower temperatures (Supplementary Figure S2A).

Stationary phase induction of SdsN is dependent on σ^S

The stationary phase induction of SdsN suggested regulation by σ^S. To investigate this possibility, we examined the SdsN levels in an *rpoS* deletion strain. Northern analysis showed that the levels of all SdsN transcripts are significantly lower in an Δ*rpoS* mutant strain in both LB (Supplementary Figure S2B) and M63 glucose medium (Figure 2B), indicating SdsN is indeed a σ^S-dependent sRNA. Consistent with the northern analysis, expression from the P_{sdsN}-*lacZ* fusion also was decreased in the *rpoS* mutant strain (Supplementary Figure S2A).

We also compared the levels of SdsN with the levels of the other known σ^S–dependent sRNAs (12–14). Interestingly, the expression patterns are not identical, and do not necessarily correlate with the highest levels of σ^S (Figure 1B). In LB, the levels of SdsN, GadY and SraL begin to increase at $OD_{600} \approx 3$ and are highest at $OD_{600} \approx 5$, while the levels of SdsR increase and peak at later time points. In M63 glucose medium, the peak of GadY expression is much earlier than

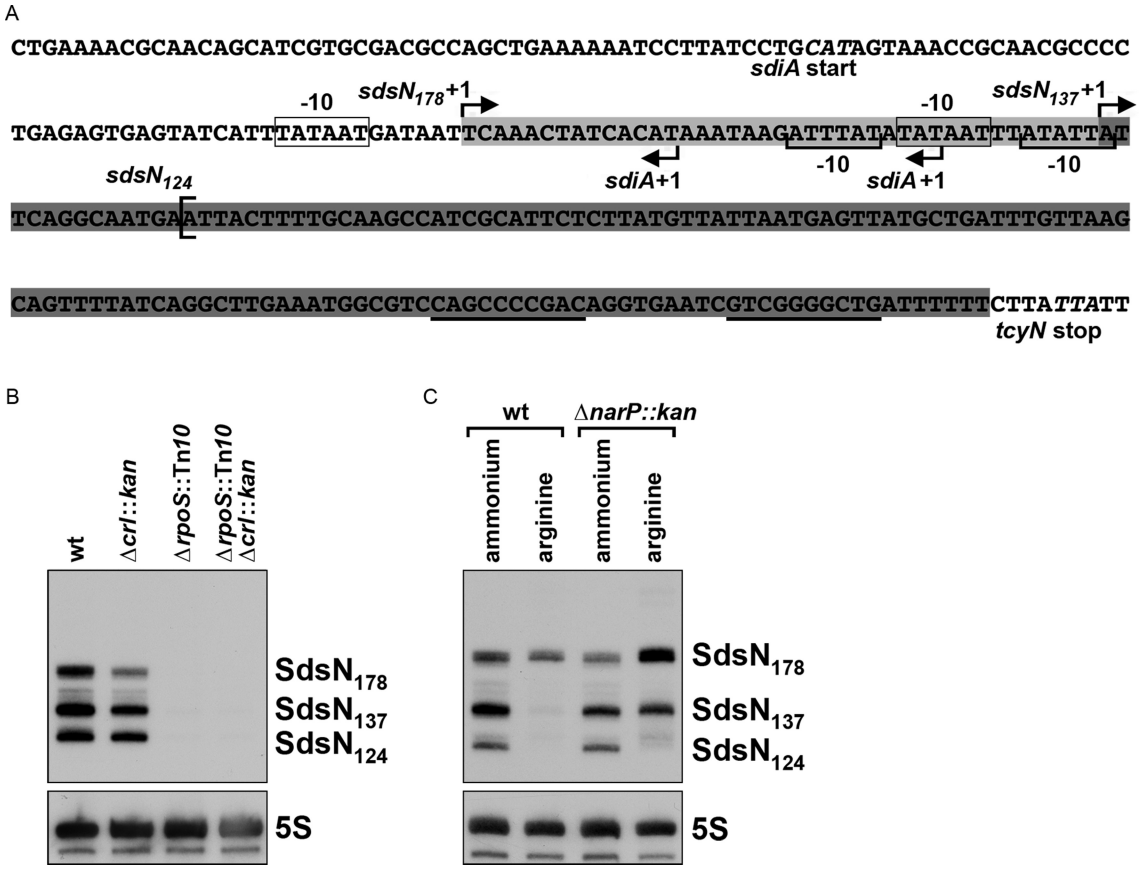

Figure 2. SdsN expression is dependent on σ^S. (**A**) Sequence of *sdsN* and *sdsN-sdiA* promoter region. The sequence that is common to $SdsN_{178}$ and $SdsN_{137}$ is shaded in dark grey, while the sequence specific to $SdsN_{178}$ is shaded in light grey. The mapped transcription start sites of $SdsN_{178}$ and $SdsN_{137}$ are indicated with arrows that show the direction of transcription; the corresponding −10 sequences are boxed. Two transcription start sites for the *sdiA* gene are also indicated with arrows that show the direction of transcription. The −10 elements for both *sdiA* transcription start sites are denoted with brackets. The 5′ end of $SdsN_{124}$ is also indicated with a vertical bracket. The *sdiA* start and *tcyN* stop codons are italicized, and the sequences corresponding to the stem of the SdsN terminator are underlined. (**B**) Levels of SdsN in WT, Δ*crl*, Δ*rpoS*, and Δ*rpoS* Δ*crl* cells. Total RNA was isolated from WT MG1655 and the isogenic Δ*crl*::*kan* (GSO760), Δ*rpoS*::Tn*10* (GSO108) and Δ*crl*::*kan* Δ*rpoS*::Tn*10* (GSO761) mutants grown 20 h in M63 glucose media (to OD_{600} ≈ 2.39, 2.40, 2.48 and 2.45, respectively) and analyzed as in Figure 1. (**C**) Effect of non-preferred and preferred nitrogen sources on SdsN levels. WT MG1655 and Δ*narP* mutant (GSO763) cells were grown 20 h in M63 glucose with preferred ammonium (15 mM) or non-preferred arginine (0.2%) as the sole nitrogen source (to OD_{600} ≈ 3.61 and 2.36, respectively for wild-type cells and OD_{600} ≈ 3.62 and 2.76 for the Δ*narP* mutant cells). RNA was processed for northern analysis as in Figure 1.

the peaks for SdsN, SraL and SdsR. Furthermore, there is limited sequence similarity among the *sdsN*, *gadY*, *sdsR* and *sraL* promoters (Supplementary Figure S2C). These observations suggest additional factors may modulate the transcription of SdsN as well as the other σ^S-dependent sRNAs or σ^S is acting indirectly, possibly by modulating sRNA stability.

σ^S-dependent induction of SdsN is impacted by nitrogen availability

Given the partial match to the consensus σ^S promoter (Supplementary Figure S2C) and *sdsN-lacZ* induction at low temperature (Supplementary Figure S2A), we considered the possibility that expression might be influenced by the Crl assembly factor, which stimulates σ^S binding to RNA polymerase and thus enhances expression from σ^S-dependent promoters when Crl levels are elevated under conditions such as low temperature (28–30). Consistent with an influence of Crl, the levels of $SdsN_{178}$ and $SdsN_{137}$ are somewhat lower in a *crl* deletion strain grown in both LB (Supplementary Figure S2B) and M63 glucose (Figure 2B) medium.

Since Crl levels are modulated by nitrogen, with reduced Crl synthesis under conditions of nitrogen limitation (30), we examined SdsN expression in cells grown in M63 glucose medium with rich and poor nitrogen sources. Growth on the preferred nitrogen source ammonium was associated with higher SdsN levels than growth on the poor nitrogen source arginine (Figure 2C). There are a number of transcription factors that regulate gene expression in response to nitrogen availability. One of these is NarP, the response regulator of the NarP-NarQ two-component system, which mediates the nitrate/nitrite responsive transcriptional regulation of anaerobic respiration (31). Since we found *narP* to be a target of SdsN (see below), we considered the possibility of a feedback loop and examined SdsN levels in a Δ*narP* background (Figure 2C). We did not observe a significant difference between the two strains grown with ammonium,

Table 1. Transcripts changed more than 2-fold upon $SdsN_{137}$ overexpression

Gene	Function	Array 1	Array 2
**nfsA*	Oxygen-insensitive nitroreductase	7.7↓	2.7↓
**ybjC*	Predicted oxidase co-transcribed with *nfsA*	2.4↓	2.6↓
**hmpA*	NO dioxygenase, flavohemoglobin	2.9↓	2.3↓
**narP*	Nitrate/nitrite response regulator	2.6↓	2.7↓
cyaY	Frataxin homolog with role in iron-sulfur cluster assembly	2.5↓	2.6↓
**uraA*	High-affinity uracil/protein symport system	2.6↓	2.2↓
**inaA*	Induced by low pH	2.1↓	2.2↓
rluA	23S rRNA and tRNA pseudouridine synthase	2.0↓	2.0↓
fliC	Flagellin	2.1↑	2.6↑
ymfT	Predicted DNA-binding transcription regulator, e14 phage	2.5↑	3.2↑

Arrows indicate genes repressed (↓) or induced (↑) upon $SdsN_{137}$ overexpression. mRNAs for genes marked with an astericks (*) are bound by Hfq (20). Annotation of function is from Ecocyc.org (52).

but interestingly, the levels of $SdsN_{178}$ and $SdsN_{137}$ were elevated, and the level of $SdsN_{124}$ was reduced in the Δ*narP* strain grown with arginine.

Given the proximity between *sdsN* and *sdiA* and reports of SdiA autoregulation (32), we also wondered whether the LuxR-type SdiA transcription factor impacts SdsN levels. Primer extension analysis (Supplementary Figure S3A) and dRNA-seq data (27) revealed two *sdiA* transcription start sites. These are both absent in an Δ*sdiA* background but differ from the previously reported starts (33), which we still detect in the Δ*sdiA* mutant and thus are likely to be artifacts (Supplementary Figure S3B). Both of the corresponding promoters overlap the *sdsN* promoters (Figure 2A). We examined the levels of SdsN in two Δ*sdiA* backgrounds but did not find a significant difference in SdsN expression under the conditions tested (Supplementary Figure S3C).

$SdsN_{137}$ and $SdsN_{178}$ bind the RNA chaperone Hfq with different affinities

Energetically favorable secondary structures of $SdsN_{137}$ (Figure 3A) and $SdsN_{178}$ (Supplementary Figure S4) were predicted using mfold (34). These predictions are supported by *in vitro* RNase T1 cleavage (Figure 3B). $SdsN_{137}$ and $SdsN_{178}$ contain the same two stem-loop structures, with the 3′ stem-loop forming the Rho-independent terminator. The 5′ AU-rich region present only on $SdsN_{178}$ appears to be largely single stranded.

While one report suggested the RNA encoded in the *sdiA-tcyN* intergenic region was bound by Hfq (25), another report showed the transcript was not stabilized by Hfq (26). To resolve this discrepancy, we subjected extracts from stationary phase cells to immunoprecipitation with either Hfq antibody or preimmune serum. Total RNA from WT and *hfq* mutant cells as well as immunoprecipitated RNA were probed for SdsN. The different forms of SdsN were all absent in the *hfq* mutant strain and all were enriched by immunoprecipitation with Hfq. However, we observed stronger enrichment for $SdsN_{178}$ than for $SdsN_{137}$ or $SdsN_{124}$ (Figure 3C). The enhanced Hfq binding to $SdsN_{178}$ relative to $SdsN_{137}$ *in vivo* was also observed in an EMSA *in vitro* binding assay in which increasing amounts of purified Hfq were added to radiolabeled $SdsN_{137}$ or $SdsN_{178}$ in the presence of an excess of competitor RNA (Figure 3D). The addition of Hfq to both sRNAs resulted in two shifts in mobility (complex I and II), similar to what is observed upon Hfq binding to other sRNAs (35). The dissociation constant (K_d) for RNA bound to Hfq in complex I, was calculated to be ∼80 nM for $SdsN_{137}$ and ∼28 nM for $SdsN_{178}$, comparable to the 25 nM K_d observed for DsrA and RprA using the same assay (35). Together these results show Hfq binds $SdsN_{178}$ with higher affinity than $SdsN_{137}$ *in vivo* and *in vitro*. Structure probing carried out after incubating $SdsN_{138}$ and $SdsN_{178}$ with Hfq (Figure 3B), showed one region of protection (G96 G97 G99) for $SdsN_{138}$, and two regions for $SdsN_{178}$ (same region between two stem-loops and another in the 5′ extension).

$SdsN_{137}$ targets mRNAs encoding proteins involved in the metabolism of and response to nitrogen compounds

Given $SdsN_{137}$ and $SdsN_{178}$ association with Hfq, we postulated the sRNAs were acting to modulate expression by basepairing with target mRNAs. To identify possible targets, we examined the genome-wide changes in RNA levels upon short-term overproduction of either $SdsN_{137}$ or $SdsN_{178}$. Exponentially-growing MG1655 cells carrying the pBR vector control, pBR-$SdsN_{137}$ or pBR-$SdsN_{178}$ were induced with 100 μM IPTG for 5 min after which total RNA was isolated and analyzed on microarrays (Supplementary Table S4). Table 1 lists genes showing greater than two-fold changes upon $SdsN_{137}$ overexpression in the two independent experiments.

$SdsN_{137}$ overexpression led to the repression of three mRNAs encoding proteins associated with the metabolism of and response to nitrogen compounds: *nfsA* encodes an oxygen-insensitive NADPH-dependent nitroreductase that catalyzes the reduction of a nitrogroup (NO_2) in nitroaromatic compounds to an amino group (NH_2) (36), and *hmpA* encodes flavohemoglobin with nitric oxide (NO) dioxygenase activity under aerobic conditions and reductase activity under anaerobic conditions (37). *ybjC*, which encodes a predicted oxidoreductase, is co-transcribed with *nfsA*, indicating that the products of these two genes may have related physiological functions. A third mRNA whose levels are repressed by $SdsN_{137}$ encodes the response regulator NarP (31).

The other transcripts whose levels were changed by $SdsN_{137}$ overproduction did not fall into a single category (*cyaY*, *uraA*, *inaA* and *rluA* were down-regulated and *fliC* and *ymfT* were up-regulated). We generated *lacZ* fusions to *cyaY*, *uraA* and *inaA* as described for *nfsA*, *hmpA* and *narP*

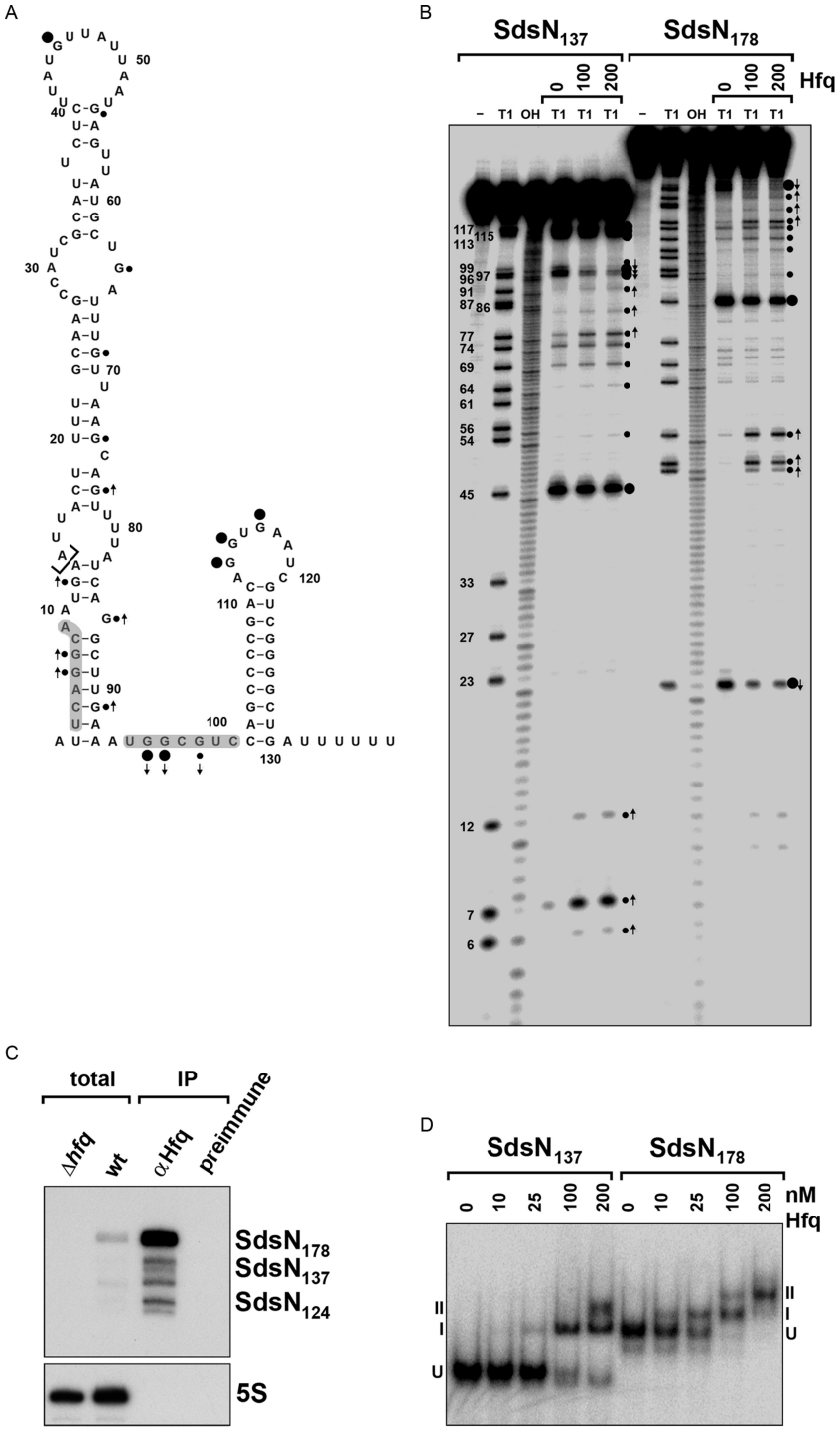

Figure 3. Both $SdsN_{137}$ and $SdsN_{178}$ bind Hfq. (**A**) Structure of $SdsN_{137}$ predicted by the mfold algorithm (34). Sites of RNase T1 cleavage as determined from Figure 3B are indicated by solid black dots with the size of the dots proportional to the amount of cleavage. Arrows indicate enhanced (↑) or repressed (↓) cleavage when RNA is pre-mixed with the indicated amounts of purified Hfq hexamer. The 5′ end of $SdsN_{124}$ is indicated with a vertical bracket. Regions involved in base pairing with *narP* at 5′ end and with *nfsA* and *hmpA* between two stem-loops are shaded. (**B**) Probing of $SdsN_{137}$ and $SdsN_{178}$ structures. Purified ^{32}P end-labeled $SdsN_{137}$ and $SdsN_{178}$ were incubated with RNase T1 (Ambion) and, for indicated samples, 100 or 200 nM purified Hfq protein and run on an 8% polyacrylamide-7M urea sequencing gel. RNase T1 and OH ladders are shown. Sites of RNase T1 cleavage are indicated as in Figure 3A. (**C**) SdsN co-immunoprecipitation with Hfq. Cell extracts were prepared from WT MG1655 grown in LB to early stationary phase ($OD_{600} \approx 5$) and subject to immunoprecipitation with α-Hfq or preimmune serum. Northern analysis was carried out on the immunoprecipitated samples (1 μg RNA loaded) as well as on total RNA (10 μg RNA loaded) isolated from WT MG1655 and the isogenic Δ*hfq*::*cat-sacB* mutant (GSO748). (**D**) $SdsN_{137}$ and $SdsN_{178}$ both bind Hfq *in vitro*. Purified ^{32}P end-labeled $SdsN_{137}$ and $SdsN_{178}$ (4 nM) were incubated with the indicated amounts of purified Hfq hexamer for 15 min at 37°C. Samples were run on a native 6% polyacrylamide gel. Unbound, complex I and complex II are indicated by U, I and II, respectively. The intensities for the bands in each lane were determined using Multi Gauge Imaging Software V3.0. K_d values were computed by plotting the appearance of protein–RNA complexes as a function of Hfq_6 concentration using the saturation-binding feature of GraphPad Software.

below. However, we did not detect expression from the *inaA* fusion, and the *cyaY* and *uraA* fusions showed no regulation by $SdsN_{137}$ (data not shown).

Interestingly, $SdsN_{178}$ overproduction did not affect any of the genes modulated by $SdsN_{137}$ (data not shown). In fact, only one mRNA, *casA* encoding a subunit of CRISPR-associated complex, showed a 2-fold increase in levels upon $SdsN_{178}$ overproduction in the two experiments.

$SdsN_{137}$ base pairs directly with *nfsA*, *hmpA* and *narP* mRNAs

The *ybjC-nfsA*, *hmpA* and *narP* mRNAs all co-immunoprecipitate with Hfq (20) and are predicted to have complementarity with $SdsN_{137}$ (Figure 4A, C and E) by the IntaRNA base pairing prediction program (38,39). For *nfsA* and *hmpA*, the predicted pairing is with the internal region of $SdsN_{137}$ shown to be single stranded by structure probing of $SdsN_{137}$ (Figure 3A and B). For *narP*, the predicted pairing is at the base of the 5′ stem, though this region is likely to be partially single stranded, as is the case for the FnrS 5′ stem (6). To test whether $SdsN_{137}$ directly base pairs with these targets, we constructed chromosomal *lacZ* fusions with the 5′ UTR as well as first nine codons of *nfsA* and *hmpA* and the first 30 codons of *narP* fused to the tenth codon of *lacZ*, all transcribed from the heterologous arabinose-inducible P_{BAD} promoter (21). As shown in Figure 4, all of the target-*lacZ* fusions were repressed 1.6- to 3-fold by $SdsN_{137}$ overexpression compared to the vector control. Mutations were introduced into the two regions of $SdsN_{137}$ predicted to pair with the *nfsA*, *hmpA* and *narP* mRNAs. Consistent with the predictions, the *nfsA-lacZ* and *hmpA-lacZ* fusions were not repressed by $SdsN_{137}$-2 (Figure 4B and D), while *narP-lacZ* was not repressed by $SdsN_{137}$-1 (Figure 4F) but was repressed by $SdsN_{137}$-2 (data not shown). However, repression was regained for fusions carrying compensatory mutations, *nfsA-2-lacZ*, *hmpA-2-lacZ* and *narP-1-lacZ*, that restore base pairing with the $SdsN_{137}$ mutants (Figure 4B, D and F). These results confirm direct base pairing between $SdsN_{137}$ and the *hmpA*, *nfsA* and *narP* mRNAs, and show that $SdsN_{137}$ utilizes at least two different regions to regulate targets.

$SdsN_{137}$ protects against nitrofurans

Previous studies have shown that the NfsA nitroreductase sensitizes *E. coli* cells to nitrofurans, nitrogen compounds that contain one or more nitrogen groups on a nitroaromatic backbone, and that cells lacking NfsA are resistant to these antibiotics (40,41). To test whether SdsN regulation of *nfsA* affects the sensitivity to these compounds, we treated LB-grown cells with 1 mM of the nitrofurans nitrofurazone or azomycin for 1 h. Overexpression of $SdsN_{137}$ led to more resistance to these antibiotics than the vector control, $SdsN_{178}$ or $SdsN_{137}$-2, the mutant unable to regulate *nfsA-lacZ* (Figure 5A and Supplementary Figure S5A). $SdsN_{137}$ did not confer further resistance to nitrofurazone in a Δ*nfsA* background (Supplementary Figure S5B).

We also examined the sensitivity of WT and Δ*sdsN* mutant cells grown 14 h in M63 glucose medium, when SdsN levels are high, to a 1 h-exposure to 2 mM nitrofurazone. Consistent with chromosomally-expressed SdsN contributing to resistance against oxidized nitrogen compounds, we always observed fewer colonies for the Δ*sdsN* mutant strain than the WT parent strain after treatment with nitrofurazone (Figure 5B).

5′ end of $SdsN_{178}$ inhibits regulation

We noted that none of the mRNAs showing regulation by $SdsN_{137}$ in the microarray experiments were affected by $SdsN_{178}$ overexpression. Since the two regions of $SdsN_{137}$ involved in base pairing with *nfsA*, *hmpA* and *narP* are contained in $SdsN_{178}$, we tested whether $SdsN_{178}$ regulates the corresponding *lacZ* fusions. As seen in Figure 6A, $SdsN_{178}$ was less effective at repressing all three fusions, particularly *narP-lacZ*.

To elucidate what sequences present in $SdsN_{178}$ reduce regulatory function, we constructed a number of deletion, mutant and chimeric derivatives of $SdsN_{178}$. The 5′ end sequence of $SdsN_{178}$ is extremely AU rich, and previous studies have shown AU-rich sequences are preferentially bound by Hfq and cleaved by RNase E (4). We first generated a series of 5′-truncations of $SdsN_{178}$ and assayed *narP-lacZ* activity upon overexpression of these derivatives (Figure 6B). All of the truncations were less effective than $SdsN_{137}$ at repressing the *narP-lacZ* fusion, including the shortest truncation $SdsN_{140}$, which is only three nucleotides longer than $SdsN_{137}$. We further mutated the three AU residues at the 5′ end of $SdsN_{140}$ by changing the residues to GC-rich sequences (AUU to CGG or GGG). With these changes, both of the mutants repress *narP-lacZ* as well as $SdsN_{137}$ (Figure 6C). It is possible some of the defects in regulation are due to somewhat lower levels of the mutant derivatives (Supplementary Figures S6A and S6B), but the sRNAs expressed from the plasmids are in vast excess. We also fused the 5′ end of $SdsN_{178}$ (nt 1–41) to the 5′ ends of the well-characterized RyhB and FnrS sRNAs, which both repress *sodB*. The addition of the SdsN sequence to both sRNAs caused a reduction in sRNA-mediated repression of a *sodB-lacZ* translational fusion despite similar sRNA levels (Supplementary Figure S6C and S6D). Interestingly, we found RyhB also represses the *narP-lacZ* fusion (Figure 6D). This regulation likely is via direct base pairing, given extensive predicted pairing (Supplementary Figure S6E) and high expression of the *narP-lacZ* fusion in a Δ*hfq* mutant, consistent with repression by multiple sRNAs (Supplementary Figure S6F). As for $SdsN_{178}$, the chimeric form of RyhB did not repress the *narP-lacZ* fusion (Figure 6D). The appended SdsN sequence could alter the structures of base pairing regions of RyhB and FnrS, but because the SdsN 5′ sequence reduces the activities of both sRNAs and the retention of base pairing has been surprisingly robust in other chimeric sRNAs (24), we do not think an altered structure fully explains the reduced repression.

To further dissect the lack of target regulation by $SdsN_{178}$, we examined $SdsN_{137}$ and $SdsN_{178}$ base pairing with target mRNAs *in vitro*. Radiolabeled $SdsN_{137}$ and $SdsN_{178}$ were mixed with Hfq at concentrations to ensure most of the sRNAs were bound by Hfq. The addition of increasing amounts of unlabeled *hmpA* or *narP* mRNA frag-

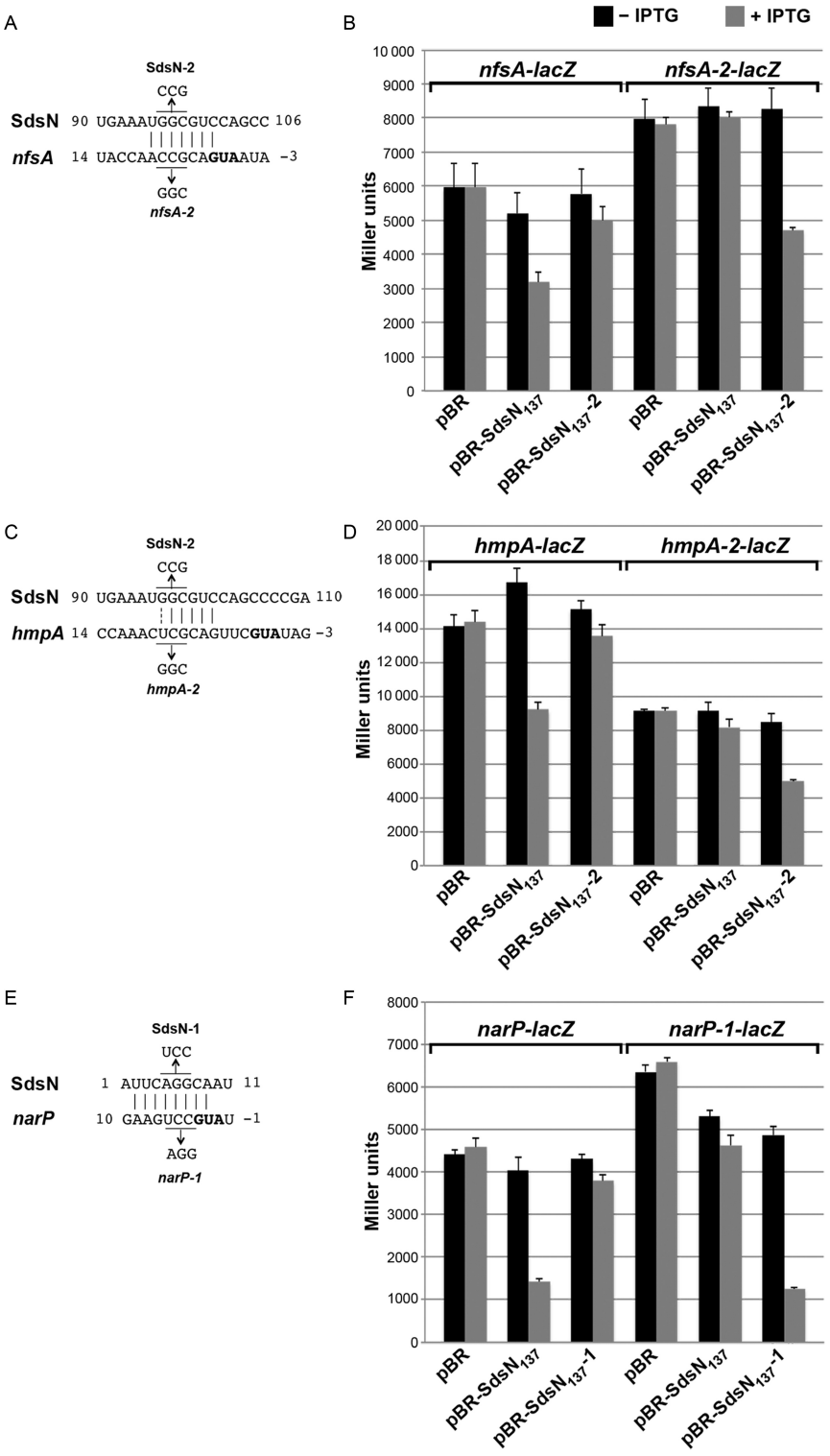

Figure 4. $SdsN_{137}$ base pairs directly with *nfsA, hmpA* and *narP*. (**A**) Predicted base pairing between SdsN and *nfsA*. The bases mutated in pBR-$SdsN_{137}$ and *nfsA* are indicated. (**B**) β-galactosidase activity of PM1205-derived strains with *nfsA-lacZ* (GSO751) or *nfsA-2-lacZ* (GSO754) carrying pBR control vector, pBR-$SdsN_{137}$ or pBR-$SdsN_{137}$ mutant derivative. (**C**) Predicted base pairing between SdsN and *hmpA*. The bases mutated in pBR-$SdsN_{137}$ and *hmpA* are indicated. (**D**) β-galactosidase activity of PM1205-derived strains with *hmpA-lacZ* (GSO752) or *hmpA-2-lacZ* (GSO755) carrying pBR control vector, pBR-$SdsN_{137}$ or pBR-$SdsN_{137}$ mutant derivative. (**E**) Predicted base pairing between SdsN and *narP*. The bases mutated in pBR-$SdsN_{137}$ and *narP* are indicated. (**F**) β-galactosidase activity of PM1205-derived strains with *narP-lacZ* (GSO753) or *narP-1-lacZ* (GSO756) carrying pBR control vector, pBR-$SdsN_{137}$ or pBR-$SdsN_{137}$ mutant derivative. For (A), (C) and (E), base pairing was predicted by IntaRNA (38,39), and numbering for mRNA is relative to start codon. For (B), (D) and (F), the levels of β-galactosidase activity of the different fusions were assayed after ∼1 h of induction with 0.2% arabinose and either 100 μM IPTG (grey bars) or no IPTG (black bars). The average values from three independent assays are shown with error bars corresponding to the standard deviation of those values.

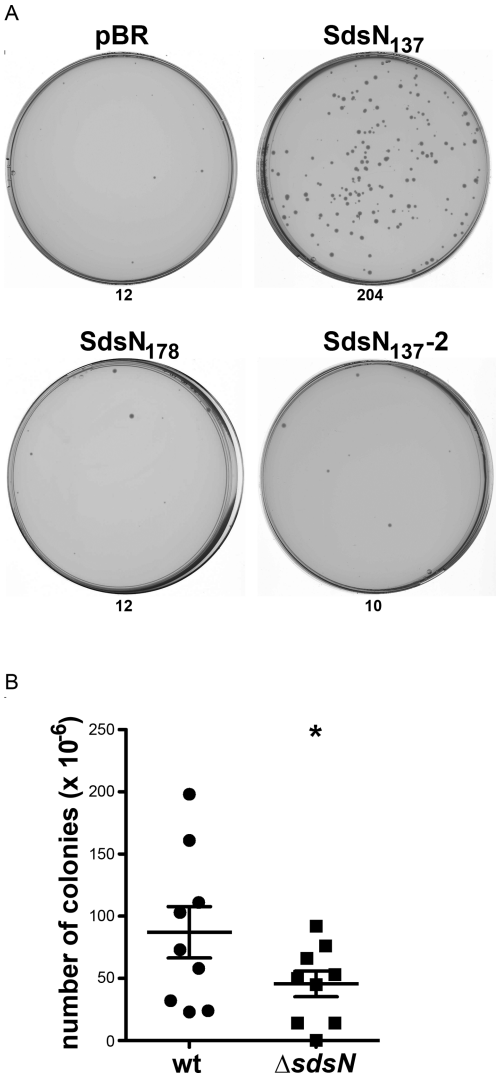

Figure 5. SdsN confers resistance to nitrofurazone. (**A**) WT MG1655 cells carrying the pBR control vector, pBR-SdsN$_{137}$, pBR-SdsN$_{178}$ or pBR-SdsN$_{137}$-2 were grown in LB supplemented with 100 μM IPTG and 100 μg/ml amp to OD$_{600}$ ≈ 0.3. Nitrofurazone was added to a final concentration of 1 mM to each culture. After 1 h at 37°C, cultures were serial diluted and plated on LB plates. The number of colonies is given below each plate. (**B**) WT MG1655 and the corresponding Δ*sdsN* strain (GSO762) were grown in M63 glucose medium for 14 h. Nitrofurazone was added to a final concentration of 2 mM. After 1 h at 37°C, cultures were again serial diluted and plated on LB plates. The data shown are for assays carried out on three separate days, each time for three independent cultures. Statistical significance (*) was calculated using an unpaired, one-tailed T-test with both data sets ($P_{value} = 0.048$).

ments to the SdsN$_{137}$-Hfq complex led to ternary complexes formed between Hfq, SdsN$_{137}$ and *hmpA* or *narP* (Figure 6E). In contrast, no ternary complex was observed when the mRNA fragments were added to SdsN$_{178}$-Hfq, even at the highest concentration of unlabeled RNA (Figure 6F).

Cleavage leads to SdsN$_{124}$ capable of regulating *hmpA* and *nfsA*

For cells grown to late stationary phase in M63 glucose medium, the levels of a third transcript, SdsN$_{124}$, were high (Figure 1B). This derivative is derived from processing given the transcript is eliminated when cells are treated with terminator exonuclease (Supplementary Figure S1C). Since a band corresponding to SdsN$_{124}$ can be detected when SdsN$_{178}$ or SdsN$_{137}$ are overexpressed from a plasmid (Figure 7A), we suggest that this derivative can be derived from either of the longer sRNAs. To test whether SdsN$_{124}$ can serve as a regulator, we again assayed the *lacZ* fusions (Figure 7B). As expected, given that SdsN$_{124}$ lacks the region for base pairing with *narP*, this fusion was not affected by SdsN$_{124}$ overexpression. In contrast, SdsN$_{124}$ repressed *nfsA-lacZ* and *hmpA-lacZ* as well as or slightly better than SdsN$_{137}$.

Previous studies have shown that while all sRNAs bind to the proximal face of the Hfq hexamer, interactions with other Hfq surfaces can differ (24). Most sRNAs (Class I) also bind the rim; these contact mRNAs on the distal face and are thus stabilized by mutations of distal face residues. A subset of sRNAs (Class II) binds the distal face; these contact mRNAs on the rim and are stabilized by mutations of rim residues. Given that sRNA binding is reflected in their levels in strains expressing proximal (Q8A), rim (R16A) and distal (Y25D, K31A) face mutants of Hfq, we examined SdsN$_{178}$, SdsN$_{137}$, SdsN$_{124}$ levels in these backgrounds (Figure 7C). The low levels of SdsN$_{124}$ in the Q8A and R16A mutants together with the elevated levels in the Y25D and K31A mutant, suggest that SdsN$_{124}$ behaves like a typical Class I binding the proximal and rim surfaces, leaving the distal face free to bind the target mRNA. In contrast, SdsN$_{137}$ and SdsN$_{178}$ are present at WT levels in the rim and distal mutants and are only partially decreased in the Q8A mutant, consistent with multiple contact sites including the distal face.

DISCUSSION

The set of SdsN RNAs can be added to a growing list of σ^S-dependent sRNAs that have been characterized for *E. coli*. In addition to σ^S, we found that the Crl and NarP transcription factors impact SdsN expression. Crl is not a DNA binding protein and is not known whether σ^S and NarP directly bind to the *sdsN* promoters. There is no signal for σ^S in the *sdsN* region in a recent chromatin immunoprecipitation-sequencing experiment (42), but there also did not appear to be binding to the *gadY* and *sraL* promoters. We were intrigued to find that multiple transcripts are expressed from the *sdiA-tcyN* intergenic region. Two forms, SdsN$_{137}$ and SdsN$_{178}$, are transcribed from two different σ^S-dependent promoters but share a terminator. These forms can be processed at the 5′ end to generate SdsN$_{124}$, which accumulates maximally after 20 h growth in M63 glucose media. The relative levels of these three main transcripts vary depending on the growth condition in ways we do not yet fully understand. SdsN$_{124}$, SdsN$_{137}$ and SdsN$_{178}$ all bind Hfq but only SdsN$_{124}$ and SdsN$_{137}$ were found to be effective regulators.

σ^S-dependent sRNAs share similar and differing features

There are some interesting similarities and differences among the σ^S-dependent sRNAs. SraL and SdsR are conserved in a range of enteric bacteria, while SdsN and GadY

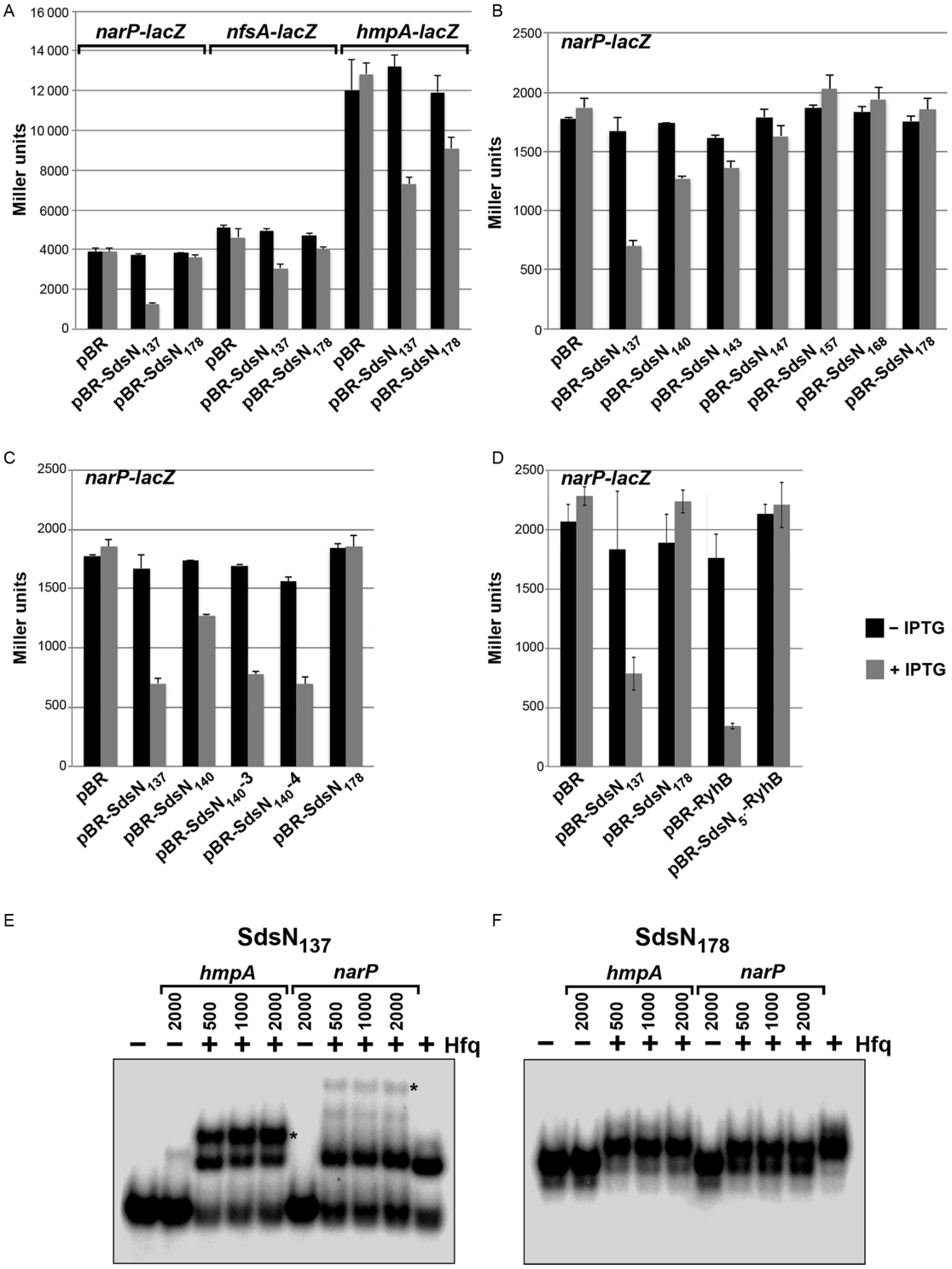

Figure 6. 5′ A- and U-rich sequences block $SdsN_{178}$ function. (**A**) β-galactosidase activity of PM1205-derived strains with *narP-lacZ*, *nfsA-lacZ* or *hmpA-lacZ* (GSO753, GSO751 and GSO752, respectively) carrying pBR control vector, pBR-$SdsN_{137}$ or pBR-$SdsN_{178}$. (**B**) β-galactosidase activity of PM1205-derived strain with *narP-lacZ* (GSO753) carrying pBR control vector, pBR-$SdsN_{137}$, pBR-$SdsN_{178}$ or plasmids with 5′ truncations of the $SdsN_{178}$. (**C**) β-galactosidase activity of PM1205-derived strain with *narP-lacZ* (GSO753) carrying pBR control vector, pBR-$SdsN_{137}$, pBR-$SdsN_{178}$, pBR-$SdsN_{140}$, pBR-$SdsN_{140}$-3 (AUU to CGG mutant) and pBR-$SdsN_{140}$-4 (AUU to GGG mutant). (**D**) β-galactosidase activity of PM1205-derived strain with *narP-lacZ* (GSO753) carrying pBR control vector, pBR-$SdsN_{137}$, pBR-$SdsN_{178}$, pBR-RyhB or pBR-$SdsN_5$′-RyhB (chimeric RyhB carrying 5′ region of SdsN). For (A), (B), (C) and (D), the levels of β-galactosidase activity of the different fusions were assayed after ∼1 h of induction with 0.2% arabinose and either 100 μM IPTG (grey bars) or no IPTG (black bars). The average values from three independent assays are shown with error bars corresponding to the standard deviation of those values. (**E**) EMSA of 4 nM of ^{32}P end-labeled $SdsN_{137}$ with 100 nM Hfq hexamer and the indicated amounts (nM) of unlabeled *hmpA* or *narP* RNA. Ternary complexes are indicated with asterisks. (**F**) EMSA of 4 nM ^{32}P end-labeled $SdsN_{178}$ with 100 nM Hfq hexamer and the indicated amounts (nM) of unlabeled *hmpA* or *narP* RNA.

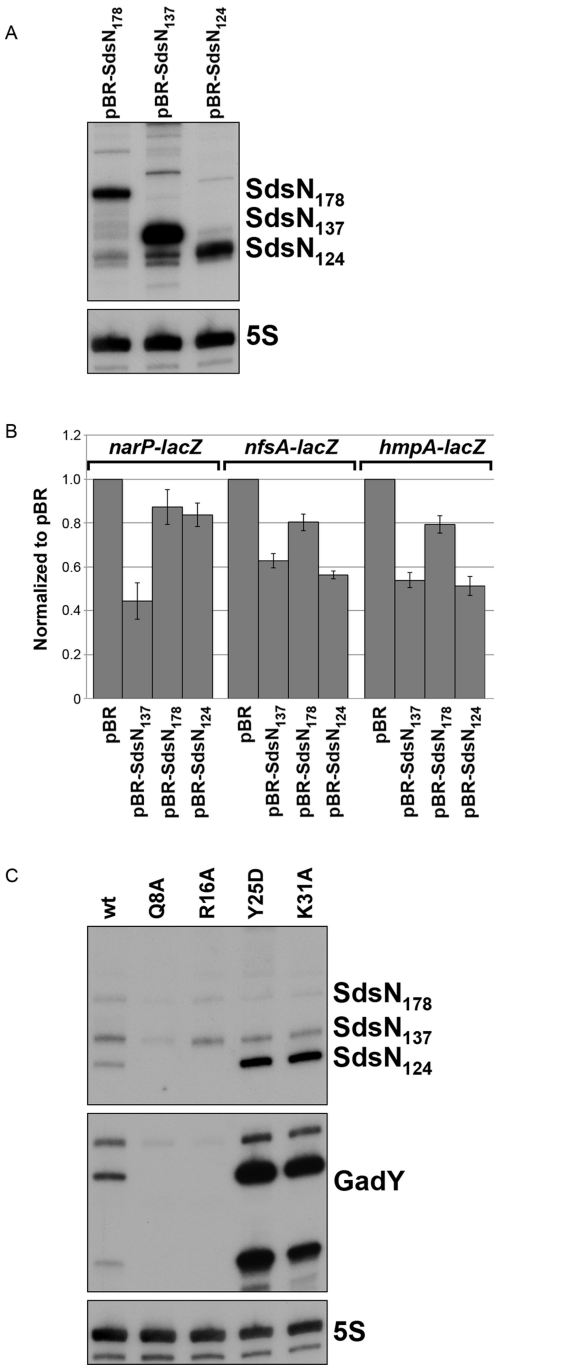

Figure 7. Cleavage activates $SdsN_{178}$. (**A**) Levels of $SdsN_{178}$, $SdsN_{137}$ and $SdsN_{124}$ expressed from pBR plasmid. Total RNA was isolated from the GSO752 cultures assayed in Figure 7B. (**B**) β-galactosidase activity of PM1205-derived strains with *narP-lacZ*, *nfsA-lacZ* or *hmpA-lacZ* (GSO753, GSO751 and GSO752, respectively) carrying pBR control vector, pBR-$SdsN_{137}$, pBR-$SdsN_{178}$ or pBR-$SdsN_{124}$. The levels of β-galactosidase activity of the different fusions were assayed after ∼3 h of induction with 0.2% arabinose and 1 mM IPTG. The average fold difference (for four independent assays) relative to the corresponding pBR vector control samples are shown with error bars corresponding to the standard deviation of the differences. (**C**) Effect of mutations affecting, rim (R16A), proximal (Q8A) and distal (Y25D, K31A) faces of Hfq. WT cells and strains expressing the indicated mutant Hfq derivatives from the chromosome (20) (DJS2317, DJS2318, DJS2319, DJS2294 and DJS2321) were grown 20 h in M63 glucose. For (A) and (C), RNA was processed for northern analysis as in Figure 1.

are restricted to *E. coli* and *Shigella*. SdsN, GadY and SdsR all strongly bind Hfq, while SraL does not. In addition, though synthesis of GadY, SraL, SdsR and SdsN is σ^S-dependent, they show different patterns of accumulation, with SdsR generally expressed later than the other sRNAs in stationary phase (Figure 1B). This observation suggests that additional factors impact the transcription or stability of the σ^S-dependent sRNAs as we found for SdsN. Little is known about what other factors might modulate GadY, SraL and SdsR levels, but it is interesting to note that overlapping transcripts are encoded on the strand opposite each of these sRNAs; *sdiA* mRNA for SdsN, *gadXW* mRNA for GadY, *soxR* mRNA for SraL and RyeA sRNA for SdsR (27).

The mRNA targets of the σ^S-dependent sRNAs do not show any functional overlap. GadY increases the synthesis of acid response transcription factors and thus may protect against low pH in stationary phase (13). The contribution of the SraL block of the translation of the Trigger Factor chaperone to stationary survival is less clear (14). SdsR represses expression of the MutS component of methyl-directed mismatch repair, possibly enhancing mutagenesis when cells are starved (16). SdsN represses genes involved in the metabolism of oxidized nitrogen compounds. By repressing the synthesis of NfsA, SdsN provides resistance to nitrofurans (Figure 5 and Supplementary Figure S5). The physiological role of SdsN repression of *hmpA* is less clear. The flavohemoglobin eliminates NO under aerobic conditions, but we did not observe any difference in NO sensitivity in the Δ*sdsN* mutant (data not shown). However the enzyme has also been shown to have other activities (43), which may be detrimental under conditions of SdsN induction.

sRNAs are induced by various nitrogen compounds

Only a few sRNAs whose expression is responsive to the levels of nitrogen compounds have been characterized in bacteria thus far (44–46). One example is RoxS from *Staphylococcus aureus* and *Bacillus subtilis*, whose transcription is induced by the presence of NO by the ResDE two-component transduction system (44). *B. subtilis* cells lacking RoxS have increased expression of genes whose functions are related to oxidative stress and oxidation-reduction reactions. Among these, the *ppnKB* mRNA encoding a NAD+/NADH kinase was confirmed to be a direct target of RoxS. However, apart from a few genes involved in the TCA cycle, there was little overlap in RoxS targets between *S. aureus* and *B. subtilis*. Another example is NrsZ from *Pseudomonas aeruginosa*, whose transcription is induced by nitrogen limitation by the NtrBC two-component transduction system (45). The only confirmed target of NrsZ, *rhlAB* encodes enzymes for the synthesis of rhamnolipid biosurfactants required for swarming motility.

Multiple forms of an sRNA allow for additional levels of regulation

$SdsN_{178}$ showed only partial regulation of *nfsA* and *hmpA* and almost no regulation of *narP* (Figure 6A), despite stronger binding to Hfq (Figure 3C and D). The secondary

structure of $SdsN_{178}$ is similar to $SdsN_{137}$ indicating the base-pairing sites should be accessible. However, the 5′ end of $SdsN_{178}$ is extremely AU-rich. *In vitro*, Hfq protects the 5′ region present on $SdsN_{178}$ from RNase T1 cleavage (Figure 3B); thus this region is an Hfq binding site not present on $SdsN_{137}$. However, we found $SdsN_{137}$ was better able to form the Hfq-sRNA-mRNA target ternary complex (Figure 6E and F) required for base pairing (47). This difference in the two forms can be explained by the 5′ end of $SdsN_{178}$ competing with the mRNA for the same surface of Hfq.

$SdsN_{124}$ represses *nfsA* and *hmpA* substantially better than $SdsN_{178}$ and slightly better than $SdsN_{137}$ (Figure 7B). The stronger regulation is not due to higher abundance since the levels of $SdsN_{124}$ are lower than $SdsN_{137}$ and equal to $SdsN_{178}$ (Figure 7A). Thus, cleavage of $SdsN_{178}$ and $SdsN_{137}$ to generate $SdsN_{124}$ probably improves base pairing with *hmpA* and *nfsA* through altered secondary structure or differences in the interaction with Hfq (Figure 7C). Cleavage also leaves a 5′-monophosphate, which may promote RNase E cleavage of the target, as was shown for MicC (48).

A number of other sRNAs have been found to be activated by post-transcriptional cleavage of the 5′ end. The first 20 nt of B. *subtilis* RoxS are removed by RNase Y generating a truncated version, which was found to be an efficient regulator *in vivo* and form a more extended duplex with the *ppnKB* mRNA *in vitro*, possibly due to disruption of the 5′ stem (44). However, the amount of this cleavage product relative to full-length is quite low under conditions tested. The two forms of *E. coli* RprA have different stabilities; the unprocessed form is subject to rapid degradation by RNase E, while the shorter cleaved form is more stable. Like SdsN, the relative levels of the two isoforms vary during growth. Intriguingly, each isoform contains seed regions responsible for regulation of different sets of mRNA targets (49). A final example is *E. coli* ArcZ (50). Again the primary transcript ($ArcZ_{121}$) is processed at the 5′ end to give a shorter form ($ArcZ_{56}$). The 5′ region of $ArcZ_{121}$ contains AU-rich sequences that are absent in $ArcZ_{56}$. As seen for SdsN, $ArcZ_{121}$ binds Hfq more tightly than $ArcZ_{56}$, *in vivo*, but $ArcZ_{56}$ forms a more stable ternary complex with Hfq and its mRNA target *in vitro*. In addition, the levels of the processed form are greatly elevated in strains expressing distal-face Hfq mutants (20), as we also observe for the cleaved derivatives of SdsN as well as GadY (Figure 7C). Given that $ArcZ_{56}$ shows greater regulation of its target than $ArcZ_{121}$, it is hypothesized that initial ArcZ expression produces a functionally inert sRNA, but is activated upon cleavage that removes the extra Hfq binding site at the 5′ end (50). We suggest that similar activation is occurring with $SdsN_{178}$. However, while $ArcZ_{121}$ is almost entirely processed under most conditions tested, $SdsN_{124}$ levels are only high in the late stationary phase in minimal media with a rich nitrogen source (Figures 1B and 2C).

We speculate additional characterization of $SdsN_{178}$, $SdsN_{137}$ and $SdsN_{124}$, as well as the processed derivatives of other sRNAs, will reveal further roles for these alternative forms. For sRNAs with multiple base pairing regions, alternative transcription and processing can lead to the regulation of different sets of target mRNAs under slightly different environmental conditions. Expression of sRNAs that bind Hfq in an inert state can prevent Hfq binding to competitor sRNAs and perhaps poise the sRNA to serve as a regulator upon cleavage in response to a specific input. These additional levels of regulation, together with tight transcriptional regulation, competition for limiting Hfq and 'sponge RNAs' described previously, illustrate the exquisite control of sRNA regulators (2,51).

SUPPLEMENTARY DATA

Supplementary Data are available at NAR Online.

ACKNOWLEDGEMENT

We thank S. Gottesman, M. Guillier and members of the Storz lab for helpful discussions and comments on the manuscript.

FUNDING

Intramural Research Program of the Eunice Kennedy Shriver National Institute of Child Health and Human Development. Funding for open access charge: ZIA [HD001608].
Conflict of interest statement. None declared.

REFERENCES

1. Storz,G., Vogel,J. and Wassarman,K.M. (2011) Regulation by small RNAs in bacteria: expanding frontiers. *Mol. Cell*, **43**, 880–891.
2. Wagner,E.G.H. and Romby,P. (2015) Small RNAs in bacteria and archaea: who they are, what they do, and how they do it. *Adv. Genet.*, **90**, 133–208.
3. Sobrero,P. and Valverde,C. (2012) The bacterial protein Hfq: much more than a mere RNA-binding factor. *Crit. Rev. Microbiol.*, **38**, 276–299.
4. Vogel,J. and Luisi,B.F. (2011) Hfq and its constellation of RNA. *Nat. Rev. Microbiol.*, **9**, 578–589.
5. Salvail,H. and Massé,E. (2012) Regulating iron storage and metabolism with RNA: an overview of posttranscriptional controls of intracellular iron homeostasis. *Wiley Interdiscip. Rev. RNA*, **3**, 26–36.
6. Durand,S. and Storz,G. (2010) Reprogramming of anaerobic metabolism by the FnrS small RNA. *Mol. Microbiol.*, **75**, 1215–1231.
7. Boysen,A., Møller-Jensen,J., Kallipolitis,B., Valentin-Hansen,P. and Overgaard,M. (2010) Translational regulation of gene expression by an anaerobically induced small non-coding RNA in *Escherichia coli*. *J. Biol. Chem.*, **285**, 10690–10702.
8. Guo,M.S., Updegrove,T.B., Gogol,E.B., Shabalina,S.A., Gross,C.A. and Storz,G. (2014) MicL, a new σE-dependent sRNA, combats envelope stress by repressing synthesis of Lpp, the major outer membrane lipoprotein. *Genes Dev.*, **28**, 1620–1634.
9. Chao,Y., Papenfort,K., Reinhardt,R., Sharma,C.M. and Vogel,J. (2012) An atlas of Hfq-bound transcripts reveals 3' UTRs as a genomic reservoir of regulatory small RNAs. *EMBO J.*, **31**, 4005–1019.
10. Battesti,A., Majdalani,N. and Gottesman,S. (2011) The RpoS-mediated general stress response in *Escherichia coli*. *Annu. Rev. Microbiol.*, **65**, 189–213.
11. Schellhorn,H.E. (2014) Elucidating the function of the RpoS regulon. *Future Microbiol.*, **9**, 497–507.
12. Fröhlich,K.S., Papenfort,K., Berger,A.A. and Vogel,J. (2012) A conserved RpoS-dependent small RNA controls the synthesis of major porin OmpD. *Nucleic Acids Res.*, **40**, 3623–3640.
13. Opdyke,J.A., Kang,J.G. and Storz,G. (2004) GadY, a small-RNA regulator of acid response genes in *Escherichia coli*. *J. Bacteriol.*, **186**, 6698–6705.
14. Silva,I.J., Ortega,A.D., Viegas,S.C., García-Del Portillo,F. and Arraiano,C.M. (2013) An RpoS-dependent sRNA regulates the expression of a chaperone involved in protein folding. *RNA*, **19**, 1253–1265.

15. Opdyke,J.A., Fozo,E.M., Hemm,M.R. and Storz,G. (2011) RNase III participates in GadY-dependent cleavage of the *gadX-gadW* mRNA. *J. Mol. Biol.*, **406**, 29–43.
16. Gutierrez,A., Laureti,L., Crussard,S., Abida,H., Rodríguez-Rojas,A., Blázquez,J., Baharoglu,Z., Mazel,D., Darfeuille,F., Vogel,J. *et al.* (2013) β-Lactam antibiotics promote bacterial mutagenesis via an RpoS-mediated reduction in replication fidelity. *Nat. Commun.*, **4**, 1610.
17. Parker,A. and Gottesman,S. (2016) Small RNA regulation of TolC, the outer membrane component of bacterial multidrug transporters. *J. Bacteriol.*, **198**, 1101–1113.
18. Datsenko,K.A. and Wanner,B.L. (2000) One-step inactivation of chromosomal genes in *Escherichiacoli* K-12 using PCR products. *Proc. Natl. Acad. Sci. U.S.A.*, **97**, 6640–6645.
19. Thomason,M.K., Fontaine,F., De Lay,N. and Storz,G. (2012) A small RNA that regulates motility and biofilm formation in response to changes in nutrient availability in *Escherichia coli*. *Mol. Microbiol.*, **84**, 17–35.
20. Zhang,A., Schu,D.J., Tjaden,B.C., Storz,G. and Gottesman,S. (2013) Mutations in interaction surfaces differentially impact *E. coli* Hfq association with small RNAs and their mRNA targets. *J. Mol. Biol.*, **425**, 3678–3697.
21. Mandin,P. and Gottesman,S. (2009) A genetic approach for finding small RNAs regulators of genes of interest identifies RybC as regulating the DpiA/DpiB two-component system. *Mol. Microbiol.*, **72**, 551–565.
22. Guillier,M. and Gottesman,S. (2006) Remodelling of the *Escherichiacoli* outer membrane by two small regulatory RNAs. *Mol. Microbiol.*, **59**, 231–247.
23. Massé,E., Escorcia,F.E. and Gottesman,S. (2003) Coupled degradation of a small regulatory RNA and its mRNA targets in *Escherichia coli*. *Genes Dev.*, **17**, 2374–2383.
24. Schu,D.J., Zhang,A., Gottesman,S. and Storz,G. (2015) Alternative Hfq-sRNA interaction modes dictate alternative mRNA recognition. *EMBO J.*, **34**, 2557–2573.
25. Zhang,A., Wassarman,K.M., Rosenow,C., Tjaden,B.C., Storz,G. and Gottesman,S. (2003) Global analysis of small RNA and mRNA targets of Hfq. *Mol. Microbiol.*, **50**, 1111–1124.
26. Raghavan,R., Groisman,E.A. and Ochman,H. (2011) Genome-wide detection of novel regulatory RNAs in *E. coli*. *Genome Res.*, **21**, 1487–1497.
27. Thomason,M.K., Bischler,T., Eisenbart,S.K., Förstner,K.U., Zhang,A., Herbig,A., Nieselt,K., Sharma,C.M. and Storz,G. (2015) Global transcriptional start site mapping using differential RNA sequencing reveals novel antisense RNAs in *Escherichia coli*. *J. Bacteriol.*, **197**, 18–28.
28. Bougdour,A., Lelong,C. and Geiselmann,J. (2004) Crl, a low temperature-induced protein in *Escherichia coli* that binds directly to the stationary phase sigma subunit of RNA polymerase. *J. Biol. Chem.*, **279**, 19540–19550.
29. Gaal,T., Mandel,M.J., Silhavy,T.J. and Gourse,R. (2006) Crl facilitates RNA polymerase holoenzyme formation. *J. Bacteriol.*, **188**, 7966–7970.
30. Zafar,M.A., Carabetta,V.J., Mandel,M.J. and Silhavy,T.J. (2014) Transcriptional occlusion caused by overlapping promoters. *Proc. Natl. Acad. Sci. U.S.A.*, **111**, 1557–1561.
31. Stewart,V. (1994) Dual interacting two-component regulatory systems mediate nitrate- and nitrite-regulated gene expression in *Escherichia coli*. *Res. Microbiol.*, **145**, 450–454.
32. Sitnikov,D.M., Schineller,J.B. and Baldwin,T.O. (1996) Control of cell division in *Escherichia coli*: regulation of transcription of *ftsQA* involves both *rpoS* and SdiA-mediated autoinduction. *Proc. Natl. Acad. Sci. U.S.A.*, **93**, 336–341.
33. Yakhnin,H., Baker,C.S., Berezin,I., Evangelista,M.A., Rassin,A., Romeo,T. and Babitzke,P. (2011) CsrA represses translation of *sdiA*, which encodes the N-acylhomoserine-L-lactone receptor of *Escherichia coli*, by binding exclusively within the coding region of *sdiA* mRNA. *J. Bacteriol.*, **193**, 6162–6170.
34. Zuker,M. (2003) Mfold web server for nucleic acid folding and hybridization prediction. *Nucleic Acids Res.*, **31**, 3406–3415.
35. Updegrove,T.B. and Wartell,R.M. (2011) The influence of *Escherichia coli* Hfq mutations on RNA binding and sRNA•mRNA duplex formation in *rpoS* riboregulation. *Biochim. Biophys. Acta*, **1809**, 532–540.
36. Zenno,S., Koike,H., Kumar,A.N., Jayaraman,R., Tanokura,M. and Saigo,K. (1996) Biochemical characterization of NfsA, the *Escherichia coli* major nitroreductase exhibiting a high amino acid sequence homology to Frp, a *Vibrio harveyi* flavin oxidoreductase. *J. Bacteriol.*, **178**, 4508–4514.
37. Gardner,P.R., Gardner,A.M., Martin,L.A. and Salzman,A.L. (1998) Nitric oxide dioxygenase: an enzymic function for flavohemoglobin. *Proc. Natl. Acad. Sci. U.S.A.*, **95**, 10378–10383.
38. Wright,P.R., Georg,J., Mann,M., Sorescu,D.A., Richter,A.S., Lott,S., Kleinkauf,R., Hess,W.R. and Backofen,R. (2014) CopraRNA and IntaRNA: predicting small RNA targets, networks and interaction domains. *Nucleic Acids Res.*, **42**, W119–W123.
39. Busch,A., Richter,A.S. and Backofen,R. (2008) IntaRNA: efficient prediction of bacterial sRNA targets incorporating target site accessibility and seed regions. *Bioinformatics*, **24**, 2849–2856.
40. McCalla,D.R., Kaiser,C. and Green,M.H. (1978) Genetics of nitrofurazone resistance in *Escherichia coli*. *J. Bacteriol.*, **133**, 10–16.
41. Whiteway,J., Koziarz,P., Veall,J., Sandhu,N., Kumar,P., Hoecher,B. and Lambert,I.B. (1998) Oxygen-insensitive nitroreductases: analysis of the roles of *nfsA* and *nfsB* in development of resistance to 5-nitrofuran derivatives in *Escherichia coli*. *J. Bacteriol.*, **180**, 5529–5539.
42. Peano,C., Wolf,J., Demol,J., Rossi,E., Petiti,L., De Bellis,G., Geiselmann,J., Egli,T., Lacour,S. and Landini,P. (2015) Characterization of the Escherichia coli σ^S core regulon by Chromatin Immunoprecipitation-sequencing (ChIP-seq) analysis. *Sci. Rep.*, **5**, 10469.
43. Bonamore,A., Gentili,P., Ilari,A., Schininà,M.E. and Boffi,A. (2003) *Escherichia coli* flavohemoglobin is an efficient alkylhydroperoxide reductase. *J. Biol. Chem.*, **278**, 22272–22277.
44. Durand,S., Braun,F., Lioliou,E., Romilly,C., Helfer,A.C., Kuhn,L., Quittot,N., Nicolas,P., Romby,P. and Condon,C. (2015) A nitric oxide regulated small RNA controls expression of genes involved in redox homeostasis in *Bacillus subtilis*. *PLoS Genet.*, **11**, e1004957.
45. Wenner,N., Maes,A., Cotado-Sampayo,M. and Lapouge,K. (2014) NrsZ: a novel, processed, nitrogen-dependent, small non-coding RNA that regulates *Pseudomonas aeruginosa* PAO1 virulence. *Environ. Microbiol.*, **16**, 1053–1068.
46. Ionescu,D., Voss,B., Oren,A., Hess,W.R. and Muro-Pastor,A.M. (2010) Heterocyst-specific transcription of NsiR1, a non-coding RNA encoded in a tandem array of direct repeats in cyanobacteria. *J. Mol. Biol.*, **398**, 177–188.
47. Updegrove,T.B., Zhang,A. and Storz,G. (2016) Hfq: the flexible RNA matchmaker. *Curr. Opin. Microbiol.*, **30**, 133–138.
48. Bandyra,K.J., Said,N., Pfeiffer,V., Górna,M.W., Vogel,J. and Luisi,B.F. (2012) The seed region of a small RNA drives the controlled destruction of the target mRNA by the endoribonuclease RNase E. *Mol. Cell*, **47**, 943–953.
49. Papenfort,K., Espinosa,E., Casadesús,J. and Vogel,J. (2015) Small RNA-based feedforward loop with AND-gate logic regulates extrachromosomal DNA transfer in *Salmonella*. *Proc. Natl. Acad. Sci. U.S.A.*, **112**, E4772–E4781.
50. Soper,T., Mandin,P., Majdalani,N., Gottesman,S. and Woodson,S.A. (2010) Positive regulation by small RNAs and the role of Hfq. *Proc. Natl. Acad. Sci. U.S.A.*, **107**, 9602–9607.
51. Lalaouna,D., Carrier,M.C. and Massé,E. (2015) Every little piece counts: the many faces of tRNA transcripts. *Transcription*, **6**, 74–77.